Hindawi Publishing Corporation
Journal of Chemistry
Volume 2015, Article ID 919636, 8 pages
http://dx.doi.org/10.1155/2015/919636

Research Article

The Effects of Acid Activation on the Thermal Properties of Polyvinylpyrrolidone and Organoclay Composites

F. Kooli

Department of Chemistry, Taibah University, P.O. Box 30002, Al-Madinah Al-Munawwarah 41447, Saudi Arabia

Correspondence should be addressed to F. Kooli; fkooli@taibahu.edu.sa

Received 5 August 2014; Revised 10 November 2014; Accepted 12 November 2014

Academic Editor: Mohammad Qamar

The thermal stabilities of polyvinylpyrrolidone-organoclays or organo-acid-activated clay composites prepared by chemical exchange reactions were assessed. The raw clay mineral was acid-activated prior to expansion by cetyltrimethylammonium surfactants. The acid activation process affected the intercalated amount of cetyltrimethylammonium cations in the resulting organoclays and, thus, the amount of polyvinylpyrrolidone in the composite. The content of cetyltrimethylammonium cations decreased with the extent of acid activation. The organophilic modification of the clay mineral was an important step in the intercalation of the polyvinylpyrrolidone molecules and, thus, in the expansion of the silicate sheets from 3.80 nm to 4.20 nm. The composites exhibited better crystalline order with intense reflections at lower angles. The thermal stability of organoclays, acid-activated clays, and composites was studied using thermogravimetric analysis and *in situ* X-ray diffraction. The decomposition of intercalated surfactants occurred at lower temperatures relative to the neat surfactant salt, and the basal spacing of the organoclays (or acid-activated clays) shrunk to 2.0 nm at 215°C. However, the basal spacing of composites exhibited better stability and collapsed to 2.0 nm at 300°C. This type of material could offer an alternative stable product for engineering purposes in the design of new composites.

1. Introduction

Polymer/clay nanocomposites (PNCs) are a class of composites in which the size of a reinforcing phase is on the order of nanometres. Since the successful development of nylon 6/clay nanocomposites in 1987 [1], there has been wild-spread interest in the academic and industrial sectors to explore this new type of PNC [2]. PNCs are a novel class of polymeric materials exhibiting properties that are synergistically derived from their components [3] and show dramatic improvements in mechanical, thermal, and barrier properties [4, 5]. In some cases, new properties not observed in their components are observed in the composite material [2]. Although a minimum weight percentage (less than 10 wt%) of layered silicates is used, much less inorganic content is present relative to conventional mineral reinforced polymer composites [6]. Polymer/clay nanocomposites have enhanced environmental and thermal stability, which promotes recycling and reduces weight. Moreover, they offer corrosion resistance, noise dampening, and dimensional stability [2].

The smectite clays are the most common type of clay mineral used in nanocomposites. A layer of smectite clay is approximately 1 nm in thickness and consists of platelets of approximately 100 nm in width, representing filler with a significantly large aspect ratio with strong dispersion and cation exchange properties. Its unit crystal is composed of two crystal sheets of silica tetrahedron with one crystal sheet of alumina octahedron between them [7]. To promote exfoliation of the clay mineral and improve the compatibility between the hydrophobic polymer and the hydrophilic clay, quaternary and alkyl-ammonium salts are widely used to modify the surface chemistry of the inorganic clay mineral [8]. Previous studies suggested that the nature of the cationic surfactants was an important factor in the preparation of PCNs [9, 10]. When preparing the polymer layered silicate nanocomposites, elevated temperatures are required during fabrication for the melt intercalation and during extrusion and shaping processes. If the processing temperature is greater than the thermal stability of the organic treatment of the organoclays, decomposition will occur, which alters the

interface between the filler and the polymer. Improvement of the thermal stability of the organoclay is crucial to prepare the polymer layered silicate nanocomposites with an expanded basal spacing that are stable above 300°C [11, 12]. To achieve these goals, new approaches for the modification of clay minerals are required for both scientific research and commercialization. Efforts have been made to synthesize thermally stable organoclays based on different cations such as stibonium [13], or imidazolium [14] and phosphonium surfactants [15]. These surfactants are too expensive for commercial use. On the other hand, the chemical reactivity of the parent aluminosilicate affected the stability of the organoclays. The degradation of bound surfactants can be facilitated by their proximity to the catalytically active aluminosilicates sites [16]. This reactivity of the aluminosilicate layers could be modified by acid activation. In fact, an organo-acid-activated clay was obtained that was stable up to 400°C under specific conditions [17].

Acid activation is the treatment of the clay with a mineral acid solution; during this process, some cations are leached from the clay mineral layers with a faster dissolution rate in the octahedral layers than the tetrahedral layers. Previous studies have shown that the specific surface area and surface acidity properties of the clay minerals can be greatly increased by acid activation [18]. The organo-acid-activated clays exhibited different properties compared to the organoclays derived from raw materials without prior treatment [19].

Polyvinylpyrrolidone (PVP) is an attractive polymer for immobilizing metal nanoparticles due to the strong affinity of the pyridyl group for metals and its ability to undergo hydrogen bonding with polar species [20]. It was used as a probe to determine the fraction of montmorillonite in soil clay. This method is based on the fact that polyvinylpyrrolidone is adsorbed on the interlayer surfaces of montmorillonite, producing a first order *c*-axis spacing of 2.6 nm, while it is not adsorbed on other swelling clays [21, 22]. Materials with controlled mesoporosity were also synthesized from synthetic polyvinylpyrrolidone-clay composites [23]. The intercalation of PVP occurred to such a degree as to delaminate the layers and cause loss of stacking registry as indicated by powder XRD [24]. The presence of the PVP in the acrylated montmorillonite clays enhanced the adsorption capacity of the clay for phenolic compounds from solution, as shown by the retention percent that was as high as 98.9% [25]. Despite the PVP adsorption on smectites, no data were reported on the intercalation of PVP in the organo-acid-activated clays. In this study, we reported the preparation of organo-acid-activated clays from a cetyltrimethylammonium bromide (C16TMABr) solution. The resulting organoclays were further treated with a polyvinylpyrrolidone (PVP) solution to obtain PVP/organoclays composites. Characterization of the resulting materials was performed using different techniques, and their thermal stability was investigated by thermogravimetric analysis and *in situ* X-ray diffraction techniques at real temperatures without cooling the sample during collection of the XRD patterns.

2. Experimental Section

2.1. Materials and Preparation. The clay mineral used herein was a Ca-rich montmorillonite (STx-1, Mt) provided by the Source Clays Repository, Purdue University (USA), with a cation exchange capacity (CEC) of 84 meq/100 g. Solid C16TMABr and PVP (with an average molecular mass of 40 000) were purchased from Aldrich and used without further purification.

The preparation of acid-activated clays was reported somewhere else [17]. Briefly, the Mt was treated with a solution of sulphuric acid at 90°C for overnight at two acid/clay ratios (in weight) of 0.2 and 0.5. The resulting acid-activated clays were repeatedly washed with deionized water and dried at ambient temperature. The samples are noted as AMt02 and AMt0.5, respectively.

To prepare the organoclays, one gram of Mt or acid-activated clays was dispersed in a solution containing different amounts of C16TMABr dissolved into 25 g of deionized water. The suspension was stirred for overnight at room temperature [25]. The solid was collected by filtration and washed by deionized water. The samples will be referred to as C16TMA-Mt, C16TMA-AMt0.2, and C16TMA-AMt0.5.

The reaction with PVP was carried out at room temperature in methanol suspension at a fixed amount of PVP. A certain mass of organoclay was added to a PVP solution and stirred overnight. The resulting materials were filtered, dried, then ground in an agate mortar, and named PVP/C16TMA-Mt, PVP/C16TMA-AMt0.2, and PVP/C16TMA-AMt0.5, respectively.

2.2. Characterization. The structure of organoclays and PVP/organoclay composites was characterized by powder X-ray diffraction (XRD). The powder XRD measurements were performed on a Bruker Advance 8 diffractometer (Ni-filtered Cu-Kα radiation with 2θ scan range of 1.5–30° at room temperature, at a scanning speed of 0.5° min^{-1}). *In situ* high temperature XRD patterns between room temperature and 425°C were recorded using an Anton Parr heating stage KT450, under an air atmosphere. The EURO EA elemental analyser was used to estimate the carbon, nitrogen, and hydrogen content in the modified clay minerals; the analysis was performed in triplicate. Thermogravimetric analysis (TGA) was performed on the TA instruments calorimeter, SDT2960, under an air flow of 100 mL min^{-1} heated from 28 to 900°C at a heating rate of 5°C min^{-1}. The FTIR spectra were recorded with a Shimadzu spectrophotometer model FTIR-8400S, using KBr pellets and a resolution of 4 cm^{-1}.

3. Results & Discussion

3.1. Elemental Analysis. The C, H, and N analysis of the organoclays and the composites is presented in Table 1. The organoclay derived from Mt prior to acid activation (C16TMA-Mt) contained the highest amount of surfactants, while the lowest content of surfactant was obtained for C16TMA-AMt0.5. The C16TMA-AMt0.2 sample exhibited an

Table 1: C, H, and N analysis (% mass) of different organoclays before and after reaction with PVP solution.

Samples	CEC meq/100 g	C%	N%	H%	*Mass loss (%)
C16TMA-Mt	92	28.14	1.87	5.40	33.51
PVP/C16TMA-Mt	92	35.21	0.93	7.25	39.21
C16TMA-AMt0.2	81	21.40	0.78	4.30	25.42
PVP/C16TMA-AMt0.2	81	26.23	0.67	6.23	31.34
C16TMA-AMt0.5	64	18.26	0.68	3.88	21.73
PVP/C16TMA-AMt0.5	64	24.56	0.53	4.54	26.12

*Deduced from TGA curves.

intermediate amount of surfactants. The difference in the surfactant content was related to the decrease of the CEC values. Indeed, the CEC decreased as the extent of the acid activation was enhanced, in good agreement with the data reported in the literature [18, 25]. The decrease of the CEC values was due to leaching of cations from the layered silicates. The organic contents in the organoclay or organo-acid-activated clays exceeded the CEC values. This excess depended on the concentrations used and the counteranions of the surfactant salts [26, 27]. We noted that there was a variation between the theoretical and loaded contents of C and N%, and the loaded contents were lower than the expected values. Similar remarks were reported in many cases. After reaction with a PVP solution, the percentage of carbon content was improved, which confirmed the presence of PVP molecules in the resulting composites. Qualitatively, the C% depended on the C16TMA content, and the highest change in C% was observed for the PVP/C16TMA-Mt composite.

3.2. X-Ray Diffraction. X-ray diffraction analyses were performed to investigate the change of the basal spacing of the modified clay minerals by surfactants and PVP. The patterns are depicted in Figure 1.

The parent clay (Mt) had a basal spacing of 1.54 nm and had good stability toward the acid treatment with a certain loss in intensity of the 001 reflection in the AMt0.5 sample [25]. In general, during acid activation, the stability of the raw clay mineral depended on its geographical origin and its chemical compositions [28, 29].

The basal spacing of C16TMA-Mt depended on the initial loading concentrations of the C16TMA cations with a gradual increase in the basal spacing from 1.54 nm to 1.81 nm to 2.15 nm when using loading concentrations below 1.23 mmol g^{-1}. Then, an abrupt expansion to 3.80 nm was observed for C16TMABr at loading concentrations of 1.64 mmol g^{-1}. No further change in the basal spacing was noted for concentrations above 1.64 mmol g^{-1} [25]. In our case, we used the samples with higher basal spacing to facilitate the intercalation of PVP.

Similar expansion of the basal spacing at 3.80 nm was obtained for C16TMA-AMt0.2 when using an initial concentration of 1.64 mmol g^{-1}, indicating that the protons in the acid-activated clay were successfully replaced by C16TMA cations (Figure 1). However, the XRD pattern of C16TMA-AMt0.5 exhibited an intense reflection at 1.92 nm with less defined reflection at 3.81 nm (Figure 1). These data could indicate that the C16TMA-AMt0.5 exhibited two phases at 3.8 nm and 1.92 nm, as proposed by Karaca et al. [30]. However, in reality the reflection of 1.92 nm was the second order of the phase of 3.81 nm, as will be shown below using *in situ* XRD.

The shape of a perfect C16TMA cation is like a nail, where the long alkyl chain is "body" of the nail and the chain end is the "nail-head." The length of the C16TMA cations fully extended is estimated to be 2.20~2.23 nm [31]. A basal spacing of 3.80 nm corresponds to an interlayer gallery of 2.84 nm (taking in account that sheet thickness of Mt clay of approximately 0.96 nm), which exceeds the length of C16TMA cations. Thus, a bilayer structure was formed where the methyl chains are all-trans and tilted with respect to the layers at a 35 degree angle [32, 33].

Water-soluble polymers, such as poly(vinyl-pyrrolidone) (PVP), can easily intercalate into sodium montmorillonite without hydrophobic treatment [34, 35]. In our case, when the hydrophilic clays were treated with PVP (Mt or acid-activated clays), the clay minerals exhibited a slight increase in their basal spacing to approximately 1.60 nm under our experiment's conditions. However, the organophilic clays showed a significant swelling of the structure after PVP intercalation. The PVP molecules induced further expansion, and the basal spacing exceeded 4.3 nm (Figure 1). Similar values were reported by Li et al. [36] and Koo et al. [37] using organoclays as host materials. The increased expansion was approximately 0.5 nm, which is close to the thickness of a monolayer of PVP intercalated between the layers. The presence of PVP molecules resulted in a better structural order of the obtained composites compared to the starting organoclays (Figure 1).

3.3. FTIR Data. The FTIR spectrum of the starting clay mineral is presented in Figure 2, and it coincided well with that reported in the literature for similar materials [38]. The two intense bands at 1040 and 1090 cm^{-1} were attributed to the Si–O stretching vibrations. The additional bands at 3626 and 3440 cm^{-1} due to hydroxyl stretching vibrations were attributed to free and interlayer water molecules, and 1638 cm^{-1} was related to the (H–O–H) bending vibrations of the water molecules adsorbed on the clay mineral. Other weak bands at 915 and 840 cm^{-1} were assigned to the bending vibrations of Al–Al–OH and Al–Mg–OH hydroxyl

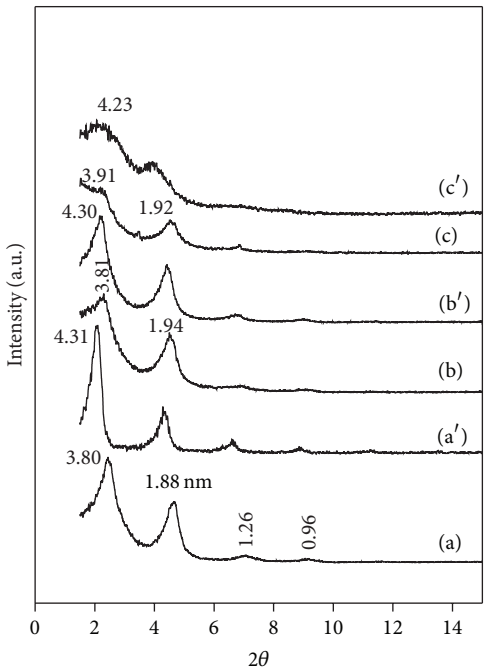

Figure 1: Powder XRD patterns of (a) C16TMA-Mt, (b) C16TMA-AMt0.2, (c) C16TMA-AMt0.5, (a′) PVP/C16TMA-Mt, (b′) PVP/C16TMA-AMt0.2, and (c′) PVP/C16TMA-AMt0.5.

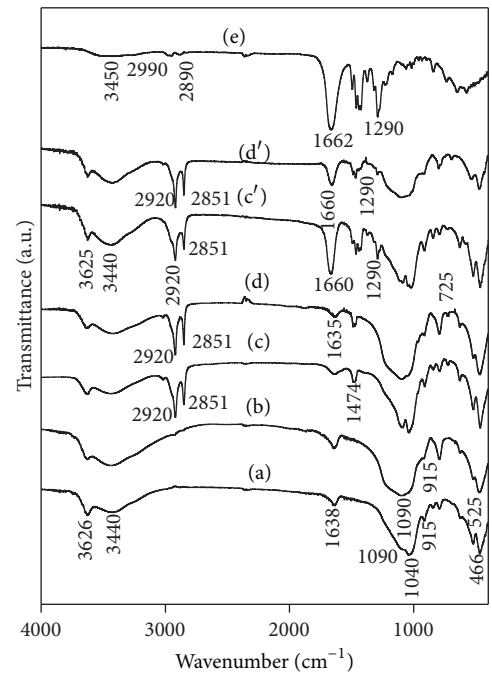

Figure 2: FTIR spectra of (a) Mt, (b) AMt0.5, (c) C16TMA-Mt, (d) C16TMA-AMt0.5 (c′) PVP/C16TMA-Mt, and (d′) PVP/C16TMA-AMt0.5. (e) The FTIR spectrum of neat PVP was presented for comparison.

groups on the edges of the clay mineral layers [39]. The Si–O–Al (octahedral Al) and Si–O–Si bending vibrations were detected at 525 and 456 cm^{-1}. In the acid-activated clays, the bands at 3626 and 1040 cm^{-1} decreased in intensity due to the destruction of the clay minerals sheets, and the band of 1090 cm^{-1} increased in intensity, due to the formation of an amorphous silica phase. The reduction in the content of the octahedral cations was accompanied by a decrease of both of the OH bending vibrations at 915 and 840 cm^{-1} [38]. After reacting with the C16TMABr solution (Figure 2), the organoclays exhibited new bands in the 2800–2950 cm^{-1} region, corresponding to antisymmetric and symmetric stretching CH_2 groups at 2920 and 2851 cm^{-1}, respectively [40]. These bands were found in all FTIR spectra of modified acid-activated clays. The bending vibrations of C–H fragments appeared at 1474 cm^{-1} [40]. The intensity of the bands in the region 2800–2950 cm^{-1} varied with the extent of acid activation, and it decreased for C16TMA-AMt0.2 and C16TMA-AMt0.5. These observations were in good agreement with the C, H, and N analysis. The bands at 1440–1480 cm^{-1} and 700–750 cm^{-1} correspond to the CH_2 scissoring and the rocking modes. These modes depended on the amine concentration, chain packing, and conformational ordering of the surfactants.

In the case of PVP, the characteristic vibration bands appeared at 1662 cm^{-1} for the C=O stretching vibration, and at 1290 cm^{-1} for the C–N stretching vibrations. The weak bands in the range of 3000 to 2080 cm^{-1} were due to antisymmetric and symmetric stretching (CH_2) of the pyrrolidone ring as well as the CH_2 groups of the backbone of the polymer. The wide adsorption band at 3450 cm^{-1} was due to OH stretching of hydrogen bonded water molecules and C–N stretching vibrations [41] (Figure 2). The FTIR spectra of the PVP/organoclays exhibited similar features (only the PVP/C16TMA-Mt spectrum is shown in Figure 2) with additional bands at 1660 cm^{-1} related to the C=O stretching mode and at 1290 cm^{-1} for the C–N stretching vibrations. We noted an improvement in intensity for the band at 3440 cm^{-1} due to the hydrogen bonding of water molecules with the PVP molecules, which was supported by the shift of the 1660 cm^{-1} band relative to the neat PVP molecules [42]. In previous works, some shifting of the Si–OH stretching band was observed; however, it was difficult to detect this shift in our experiments. The band associated with water molecules vanished, though it could be overlapped with the C=O stretching band of PVP. For the PVP/C16TMA-AMt0.2 and PVP/C16TMA-AMt0.5 samples, a decrease in the intensity of the band at 3000–3600 cm^{-1} was observed, which confirmed the less hydrogen bonding between water and the PVP molecules.

3.4. Thermogravimetric Data. Thermal degradation and stability of the intercalated organoclays were studied by conducting thermogravimetric analysis. TGA curves for the starting clays were reported in detail in our previous work [17, 25]. The starting Mt and its acid-activated counterparts exhibited two mass loss steps; the first mass loss occurring between room temperature and 110°C was attributed to the loss of physisorbed and intercalated water molecules from the interlayer spacing; the second mass loss occurring from 400 to 600°C was due to the dehydroxylation of silicate structure.

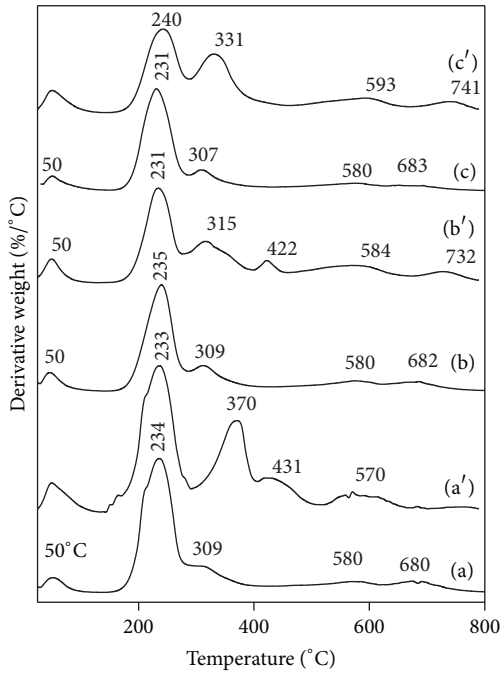

Figure 3: Derivative thermogravimetric analysis (DTG) curves of (a) C16TMA-Mt, (b) C16TMA-AMt0.2, (c) C16TMA-AMt0.5, (a′) PVP/C16TMA-Mt, (b′) PVP/C16TMA-AMt0.2, and (c′) PVP/C16TMA-AMt0.5.

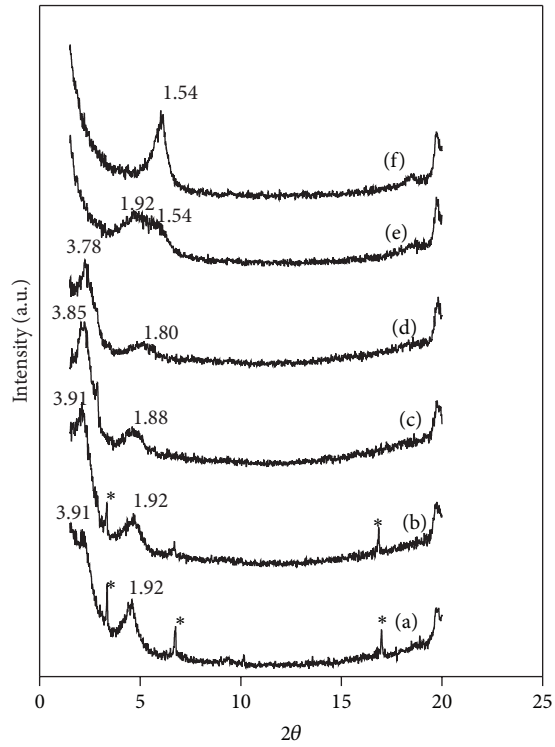

Figure 4: *In situ* XRD patterns of C16TMA-AMt0.5 calcined at different temperatures. (a) 25, (b) 100, (c) 150, (d) 200, (e) 215, (f) 250, and (g) 300°C. ∗ corresponds to C16TMABr salt as impurities.

The percentage of mass lost during the second mass loss decreased for the acid-activated clays due to the destruction of the clay mineral sheets during the acid treatment.

The neat PVP began to degrade above 270°C and was completely decomposed above 600°C [43]. It exhibited a mass loss related to release of water molecules in the range of 25 to 105°C, followed by three mass losses in the range of 270°C to 700°C associated with different decomposition steps of the polymer at different temperatures. The DTG curve exhibited two overlapping intense signals in the range of 400 to 460°C. The peak at 514°C was associated with complete burning of the residual carbonaceous material. The C16TMABr solid started to decompose at lower temperatures of 168°C in mainly two mass loss steps (Figure 2), related to degradation of the alkyl chains and burning out of the residual organic material. We noted that the decomposition of the C16TMABr mechanism depended on the atmosphere used, air or nitrogen [17], which is not the case for the PVP material.

Compared to the raw clay mineral, the organoclays exhibited an additional mass loss near 150°C that was related to the decomposition of the intercalated C16TMA cations [44]. The percentage of mass loss during decomposition of the C16TMA cations increased with the increase of C16TMA contents, and the C16TMA-Mt exhibited the highest mass loss percentage, which was in good agreement with C, H, and N analysis (see Table 1). The maximum temperature for the decomposition of the C16TMA cations in the organoclays occurred at lower temperatures relative to the pure C16TMABr salt (Figure 3). It was reported that the temperature of this decomposition is related to the basal spacing of the organoclays [40]. In our case, the value of 3.80 nm made the decomposition of the intercalated surfactants easy. We noted that the DTG of PVP/organoclays exhibited different features [45].

The DTG curve of PVP/C16TMA-Mt exhibited not only the mass loss of the C16TMA cations but also two mass losses at 370 and 431°C related to the presence of PVP in the material (Figure 3). The maximum temperature of the peak at 431°C shifted to lower temperatures for the PVP/C16TMA-AMt0.2, and it vanished for PVP/C16TMA-AMt0.5 (Figure 3).

These data indicated that the decomposition of PVP molecule was affected by the C16TMA cations contents and the acidity of the clay mineral sheets. We noted that the PVP molecules did not affect the temperature of C16TMA cations decomposition. However, complete combustion of the carbonaceous materials occurred at higher temperatures compared to the original organoclays (Figure 3). Overall, the loss of intercalated PVP molecules occurred at lower temperatures, which indicated that the interlayer space influences the decomposition steps of PVP. However, in some cases, the thermal stability of the polymer is improved due to the presence of metals as nanofillers [46].

3.5. In Situ XRD. The thermal stability of the intercalated composites suggested some preservation of the silicate structure in its expanded form. The *in situ* XRD studies of the raw Mt and AMt0.2 clays indicated that a layer of water molecules was released, which was associated with a decrease in the basal spacing to 1.25 nm at 100°C. Shrinkage of the

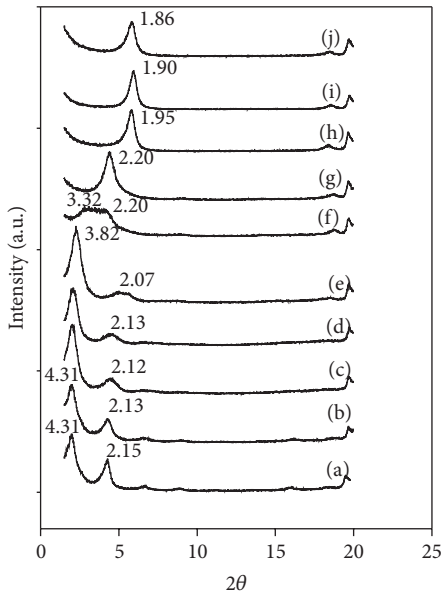

Figure 5: *In situ* XRD patterns of PVP/C16TMA-Mt composite calcined at different temperatures. (a) 25, (b) 100, (c) 150, (d) 200, (e) 205, (f) 215, (g) 250, (h) 300, (i) 350, and (j) 425 (°C).

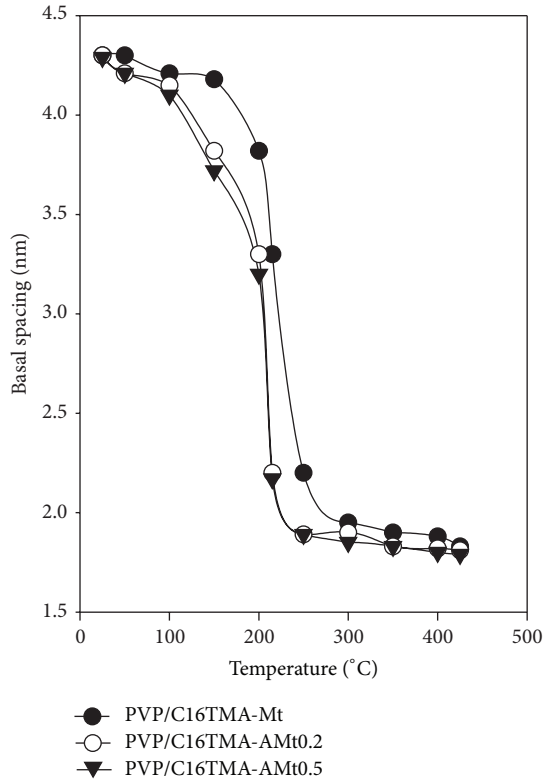

Figure 6: Variation of the basal spacing of the different materials calcined at different temperatures.

basal spacing to 0.96 nm was achieved above 100°C [16, 17]. In contrast, the AMt0.5 clay did not shrink completely and two phases at 0.96 nm and 1.36 nm were observed at temperatures above 100°C. The spacing of 1.36 nm was attributed to the presence of some silica species generated during the acid treatment [25]. The pure C16TMABr salt exhibited a layered structure with a basal spacing of 2.6 nm. This value was close to the size of the C16TMA surfactant (with some error). The basal spacing of the C16TMABr salt increased from 2.6 nm to 3.28 nm when it was heated from 25 to 215°C. Above this temperature, it was destroyed [25]. Although the DTG curve did not show a variation of mass in this range, some structural changes in the surfactant occurred. The PVP polymer at room temperature exhibited an amorphous structure, and the powder XRD pattern exhibited a broad hallow. Similar patterns were obtained when it was heated up to 250°C.

The organoclay C16TMA-Mt exhibited a stability up to 200°C, with no variation in the basal spacing. At 215°C, the spacing decreased to 2.91 nm [25]. At higher temperatures (250°C and above), the layered structure shrunk completely to a basal spacing of 1.37 nm due to the fragmentation of the intercalated surfactants. In the case of C16TMA-AMt0.2, the basal spacing of 3.80 nm decreased continuously at intermediate temperatures between 50 and 210°C from 3.80 to 1.61 nm. At temperatures above 215°C a basal spacing of 1.40 nm was obtained due to the decomposition of the organic surfactants and the presence of residual carbonaceous materials. As we have mentioned in Section 3.2, the C16TMA-Mt0.5 XRD data at room temperature could be represented in two phases. However, the *in situ* XRD data confirmed that only one phase at 3.82 nm was present, with an increase of the intensity's reflection at 3.82 nm and simultaneously shift of the two reflections (Figure 4) once calcined at different temperatures. In some cases, we noted an increase of the basal spacing of the organoclays, especially for C16TMA-Mt. This fact was related to the melting of the intercalated surfactant in its liquid state [47, 48]. Compared to pure C16TMABr, the increase of the basal spacing of the organoclay occurred in a short range of temperatures due to geometric constraining effects from the silicate layers in addition to the packing density requirements that maintain the charge neutrality [48].

After the intercalation of PVP molecules, the *in situ* XRD indicated that the basal spacing of PVP/C16TMA-Mt was stable up to 200°C, before it decreased to 2.20 nm at temperatures above 250°C (Figure 5). This value was higher than the 1.40 nm for C16TMA-Mt, which was due to the presence of the PVP molecules. The presence of PVP molecules did not cause an increase in the basal spacing in the range of 50 to 100°C compared to C16TMA-Mt precursor. At higher temperatures above 250°C, the calcined composite exhibited a basal spacing of 1.82 nm due the presence of residual carbonaceous materials resulting from both C16TMA cations and PVP molecules. The polymer composites obtained from acid-activated organoclays exhibited slightly lower stability, with a shrinkage of the basal spacing to 2.20 nm at temperatures below 250°C (Figure 6). The difference could be related to the chemical composition of clay sheets and their acidity, which affected the decomposition process of the organic compounds between the silicate sheets. Indeed, the AMt0.5 had a lower acidity value of 46 mmol of protons/g compared to AMt0.3 (70 mmol of protons/g) measured by desorption of cyclohexylamine as a probe molecule [25].

4. Conclusions

The acid activation process affected the amounts of intercalated C16TMA cations and, thus, the amount of PVP molecules. The basal spacing expanded from 1.54 nm to 3.80 nm, and this expansion depended on the initial loading concentrations of the surfactants. Further expansion was recorded when treated with the PVP solution. There was a significant difference in the thermal behaviour of the organoclays and related composites. The PVP/organoclay composites prepared from nontreated (raw) clay exhibited higher thermal stability above 250°C relative to similar material prepared from acid-activated clays. The geometric constraints due to the presence of the silicate layers in addition to the composition of the silicate layers might be the origin of such a difference, which affected the decomposition of the organic compounds.

Conflict of Interests

The author declares that there is no conflict of interests regarding the publication of this paper.

References

[1] Y. Fukushima and S. Inagaki, "Synthesis of an intercalated compound of montmorillonite and 6-polyamide," *Journal of Inclusion Phenomena*, vol. 5, no. 4, pp. 473–482, 1987.

[2] M. Alexandre and P. Dubois, "Polymer-layered silicate nanocomposites: preparation, properties and uses of a new class of materials," *Materials Science and Engineering R*, vol. 28, no. 1, pp. 1–63, 2000.

[3] A. Okada and A. Usuki, "Twenty years of polymer-clay nanocomposites," *Macromolecular Materials & Engineering*, vol. 291, no. 12, pp. 1449–1476, 2006.

[4] E. P. Giannelis, "Polymer layered silicate nanocomposites," *Advanced Materials*, vol. 8, no. 1, pp. 29–35, 1996.

[5] J.-H. Chang and Y. U. An, "Nanocomposites of polyurethane with various organoclays: thermomechanical properties, morphology, and gas permeability," *Journal of Polymer Science Part B: Polymer Physics*, vol. 40, no. 7, pp. 670–677, 2002.

[6] F. Gao, "Clay/polymer composites: the story," *Materials Today*, vol. 7, no. 11, pp. 50–55, 2004.

[7] B. Tyagi, C. D. Chudasama, and R. V. Jasra, "Determination of structural modification in acid activated montmorillonite clay by FT-IR spectroscopy," *Spectrochimica Acta Part A: Molecular and Biomolecular Spectroscopy*, vol. 64, no. 2, pp. 273–278, 2006.

[8] P. C. Lebaron, Z. Wang, and T. J. Pinnavaia, "Polymer-layered silicate nanocomposites: an overview," *Applied Clay Science*, vol. 15, no. 1-2, pp. 11–29, 1999.

[9] S. Sinha Ray and M. Okamoto, "Polymer/layered silicate nanocomposites: a review from preparation to processing," *Progress in Polymer Science*, vol. 28, no. 11, pp. 1539–1641, 2003.

[10] T. D. Fornes, P. J. Yoon, D. L. Hunter, H. Keskkula, and D. R. Paul, "Effect of organoclay structure on nylon 6 nanocomposite morphology and properties," *Polymer*, vol. 43, no. 22, pp. 5915–5933, 2002.

[11] Y. Komori and K. Kuroda, "Layered silicate-polymer interlocation composites varieties in host materials and properties," in *Polymer-Clay Nanocomposites*, T. J. Pinnavaia and G. W. Beall, Eds., pp. 3–18, John Wiley & Sons, New York, NY, USA, 2001.

[12] A. Leszczyńska, J. Njuguna, K. Pielichowski, and J. R. Banerjee, "Polymer/montmorillonite nanocomposites with improved thermal properties. Part I. Factors influencing thermal stability and mechanisms of thermal stability improvement," *Thermochimica Acta*, vol. 453, no. 2, pp. 75–96, 2007.

[13] D. Wang and C. Wilkie, "A stibonium-modified clay and its polystyrene nanocomposite," *Polymer Degradation and Stability*, vol. 82, no. 2, pp. 309–315, 2003.

[14] W. H. Awad, J. W. Gilman, M. Nyden et al., "Thermal degradation studies of alkyl-imidazolium salts and their application in nanocomposites," *Thermochimica Acta*, vol. 409, no. 1, pp. 3–11, 2004.

[15] J. U. Calderon, B. Lennox, and M. R. Kamal, "Thermally stable phosphonium-montmorillonite organoclays," *Applied Clay Science*, vol. 40, no. 1–4, pp. 90–98, 2008.

[16] W. Xie, Z. Gao, W.-P. Pan, D. Hunter, A. Singh, and R. Vaia, "Thermal degradation chemistry of alkyl quaternary ammonium Montmorillonite," *Chemistry of Materials*, vol. 13, no. 9, pp. 2979–2990, 2001.

[17] F. Kooli, Y. Z. Khimyak, S. F. Alshahateet, and F. Chen, "Effect of the acid activation levels of montmorillonite clay on the cetyltrimethylammonium cations adsorption," *Langmuir*, vol. 21, no. 19, pp. 8717–8723, 2005.

[18] K. A. Carrado and P. Komadel, "Acid activation of bentonites and polymer-clay nanocomposites," *Elements*, vol. 5, no. 2, pp. 111–116, 2009.

[19] F. Kooli, L. Yan, S. X. Tan, and J. Zheng, "Organoclays from alkaline-treated acid-activated clays: properties and thermal stability," *Journal of Thermal Analysis and Calorimetry*, vol. 115, no. 2, pp. 1465–1475, 2014.

[20] A. Slistan-Grijalva, R. Herrera-Urbina, J. F. Rivas-Silva, M. Ávalos-Borja, F. F. Castillón-Barraza, and A. Posada-Amarillas, "Synthesis of silver nanoparticles in a polyvinylpyrrolidone (PVP) paste, and their optical properties in a film and in ethylene glycol," *Materials Research Bulletin*, vol. 43, no. 1, pp. 90–96, 2008.

[21] R. Levy and C. W. Francis, "Interlayer adsorption of polyvinylpyrrolidone on montmorillonite," *Journal of Colloid And Interface Science*, vol. 50, no. 3, pp. 442–450, 1975.

[22] A. E. Blum and D. D. Eberl, "Measurement of clay surface areas by polyvinylpyrrolidone (PVP) sorption and its use for quantifying illite and smectite abundance," *Clays and Clay Minerals*, vol. 52, no. 5, pp. 589–602, 2004.

[23] K. A. Carrado and L. Xu, "Materials with controlled mesoporosity derived from synthetic polyvinylpyrrolidone-clay composites," *Microporous and Mesoporous Materials*, vol. 27, no. 1, pp. 87–94, 1999.

[24] M. Szczerba, J. Środoń, M. Skiba, and A. Derkowski, "One-dimensional structure of exfoliated polymer-layered silicate nanocomposites: a polyvinylpyrrolidone (PVP) case study," *Applied Clay Science*, vol. 47, no. 3-4, pp. 235–241, 2010.

[25] F. Kooli, Y. Liu, S. F. Alshahateet, M. Messali, and F. Bergaya, "Reaction of acid activated montmorillonites with hexadecyl trimethylammonium bromide solution," *Applied Clay Science*, vol. 43, no. 3-4, pp. 357–363, 2009.

[26] S. Y. Lee and S. J. Kim, "Expansion of smectite by hexadecyltrimethylammonium," *Clays and Clay Minerals*, vol. 50, no. 4, pp. 435–445, 2002.

[27] F. Kooli, L. S. Qin, Y. Y. Kiat, Q. Weirong, and P. C. Hian, "Effect of hexadecyltrimethylammonium (C16TMA) counteranions on the intercalation properties of different montmorillonites," *Clay Science*, vol. 12, supplement 2, pp. 325–330, 2006.

[28] P. Komadel, M. Janek, J. Madejová, A. Weekes, and C. Breen, "Acidity and catalytic activity of mildly acid-treated Mg-rich montmorillonite and hectorite," *Journal of the Chemical Society—Faraday Transactions*, vol. 93, no. 23, pp. 4207–4210, 1997.

[29] F. Kooli and L. Yan, "Chemical and thermal properties of organoclays derived from highly stable bentonite in sulfuric acid," *Applied Clay Science*, vol. 83-84, pp. 349–356, 2013.

[30] S. Karaca, A. Gürses, and M. E. Korucu, "Investigation of the orientation of CTA^+ ions in the interlayer of CTAB pillared montmorillonite," *Journal of Chemistry*, vol. 2013, Article ID 274838, 10 pages, 2013.

[31] N. V. Venkataraman and S. Vasudevan, "Conformation of methylene chains in an intercalated surfactant bilayer," *The Journal of Physical Chemistry B*, vol. 105, no. 9, pp. 1805–1812, 2001.

[32] K. Tamura and H. Nakazawa, "Intercalation of N-alkyltrimethylammonium into swelling fluoro-mica," *Clays and Clay Minerals*, vol. 44, no. 4, pp. 501–505, 1996.

[33] J. Zhu, H. He, J. Guo, D. Yang, and X. Xie, "Arrangement models of alkylammonium cations in the interlayer of $HDTMA^+$ pillared montmorillonites," *Chinese Science Bulletin*, vol. 48, no. 4, pp. 368–372, 2003.

[34] C. W. Francis, "Sorption of polyvinylpyrrolidone on reference clay minerals," *Soil Science*, vol. 115, pp. 40–54, 1973.

[35] A. Gultek, T. Seckin, Y. Onal, and M. Galip Icduygu, "Preparation and phenol captivating properties of polyvinylpyrrolidone-montmorillonite hybrid materials," *Journal of Applied Polymer Science*, vol. 81, no. 2, pp. 512–519, 2001.

[36] T. Li, X. Zeng, and J. Xu, "Preparation and characterization of conductive polypyrrole/organophilic montorillonite nanocomposite," *Polymer—Plastics Technology and Engineering*, vol. 46, no. 8, pp. 751–757, 2007.

[37] C. M. Koo, H. T. Ham, M. H. Choi, S. O. Kim, and I. J. Chung, "Characteristics of polyvinylpyrrolidone-layered silicate nanocomposites prepared by attrition ball milling," *Polymer*, vol. 44, no. 3, pp. 681–689, 2002.

[38] F. Kooli, L. Yan, S. X. Tan, and J. Zheng, "Organoclays from alkaline-treated acid-activated clays," *Journal of Thermal Analysis and Calorimetry*, vol. 115, no. 2, pp. 1465–1475, 2014.

[39] J. Madejová, M. Pentrák, H. Pálková, and P. Komadel, "Near-infrared spectroscopy: a powerful tool in studies of acid-treated clay minerals," *Vibrational Spectroscopy*, vol. 49, no. 2, pp. 211–218, 2009.

[40] J. Zhu, H. He, L. Zhu, X. Wen, and F. Deng, "Characterization of organic phases in the interlayer of montmorillonite using FTIR and ^{13}C NMR," *Journal of Colloid and Interface Science*, vol. 286, no. 1, pp. 239–244, 2005.

[41] T. Li, X. Zeng, and J. Xu, "Preparation and characterization of conductive polypyrrole/organophilic montorillonite nanocomposite," *Polymer-Plastics Technology and Engineering*, vol. 46, no. 8, pp. 751–757, 2007.

[42] D. Mondal, M. M. R. Mollick, B. Bhowmick et al., "Effect ofpoly (vinylpyrrolidone) ont hemorphology andphysicalproperties of poly (vinylalcohol)/sodium montmorillonite nanocomposite films," *Progress in Natural Science: Materials International*, vol. 23, pp. 579–587, 2013.

[43] K.-S. Chou and C.-C. Chen, "Fabrication and characterization of silver core and porous silica shell nanocomposite particles," *Microporous and Mesoporous Materials*, vol. 98, no. 1–3, pp. 208–213, 2007.

[44] Y. Park, G. A. Ayoko, J. Kristof, E. Horváth, and R. L. Frost, "A thermoanalytical assessment of an organoclay," *Journal of Thermal Analysis and Calorimetry*, vol. 107, no. 3, pp. 1137–1142, 2012.

[45] C. B. Hedley, G. Yuan, and B. K. G. Theng, "Thermal analysis of montmorillonites modified with quaternary phosphonium and ammonium surfactants," *Applied Clay Science*, vol. 35, no. 3-4, pp. 180–188, 2007.

[46] S. S. Gasaymeh, S. Radiman, L. Y. Heng, E. Saion, and G. H. M. Saeed, "Synthesis and characterization of silver/polyvinilpirrolidone (AG/PVP) nanoparticles using gamma irradiation techniques," *American Journal of Applied Sciences*, vol. 7, no. 7, pp. 879–888, 2010.

[47] M. R. Thompson, M. P. Balogh, R. L. Speer, P. D. Fasulo, and W. R. Rodgers, "In situ x-ray diffraction studies of alkyl quaternary ammonium montmorillonite in a CO_2 environment," *Journal of Chemical Physics*, vol. 130, no. 4, Article ID 044705, 2009.

[48] W. Xie, R. Xie, W.-P. Pan et al., "Thermal stability of quaternary phosphonium modified montmorillonites," *Chemistry of Materials*, vol. 14, no. 11, pp. 4837–4845, 2002.